High-dimensional mediation analysis to elucidate the role of metabolites in the association between PFAS exposure and reduced SARS-CoV-2 IgG in pregnancy

Authors: Haibin Guan[1], Jia Chen[1**], Kirtan Kaur[1], Bushra Amreen[1], Corina Lesseur[1], Georgia Dolios[1], Syam S. Andra[1], Srinivasan Narasimhan[1], Divya Pulivarthi[1], Vishal Midya[1], Lotje D. De Witte[2], Veerle Bergink[2], Anna-Sophie Rommel[2], and Lauren M. Petrick[1, 3, 4*]

[1] Department of Environmental Medicine and Climate Science, Icahn School of Medicine at Mount Sinai, New York, NY 10029, USA.
[2] Department of Psychiatry, Icahn School of Medicine at Mount Sinai, New York, NY, 10029, USA
[3] Institute for Exposomic Research, Icahn School of Medicine at Mount Sinai, New York, NY 10029, USA.
[4] The Bert Strassburger Metabolic Center, Sheba Medical Center, Tel-Hashomer, Israel.

*Corresponding author, Email address: lauren.petrick@mssm.edu
**Corresponding author, Email address: jia.chen@mssm.edu

Abstract

Objective: We previously found that per- and polyfluoroalkyl substances (PFAS) mixture exposure is inversely associated with SARS-CoV-2 IgG (IgG) antibody levels in pregnant individuals. Here, we aim to identify metabolites mediating this relationship to elucidate the underlying biological pathways. **Methods:** We included 59 pregnant participants from a US-based pregnancy cohort. Untargeted metabolomic profiling was performed using Liquid Chromatography-High Resolution Sass spectrometry (LC-HRMS), and weighted Quantile Sum (WQS) regression was applied to assess the PFAS and metabolites mixture effects on IgG. Metabolite indices positively or negatively associated with IgG levels were constructed separately and their mediation effects were examined independently and jointly. **Results**: The PFAS-index was negatively associated with IgG levels (beta=-0.273, p=0.002), with PFHpS and PFHxS as major contributors. Two metabolite-indices were constructed, one positively (beta=1.260, p<0.001) and one negatively (beta=-0.997, p<0.001) associated with IgG. Key contributors for these indices included protoporphyrin, 5-hydroxytryptophan, n-acetylproline, and tyrosine. Analysis of single mediator showed that 48.9% (95%CI: 21.9%,125.0%) and 50.1% (95% CI: 8.1%, 90.1%) of the PFAS index-IgG total effect were mediated by the negative and positive metabolite-indices, respectively. Joint analysis of the metabolite-indices indicated a cumulative mediation effect of 73.6% (95%CI: 44.9%, 116.4%). Enriched pathways associated with these metabolites indices were phenylalanine, tyrosine, and tryptophan biosynthesis and arginine metabolism. **Conclusions:** We observed significant mediation effects of plasma metabolites on the PFAS-IgG relationship, suggesting that PFAS disrupts the balance of plasma metabolites that contributes to reduced plasma IgG production.

Keywords

Exposome, per- and polyfluoroalkyl substances (PFAS), mixture modelling, weighted quantile sum regression, metabolomics, SARS-CoV-2 IgG antibody, mediation analysis

Introduction

PFAS (Per- and Polyfluoroalkyl Substances), often called "forever chemicals," are industrial chemicals widely used due to their durability. Their extensive use and tendency to bioaccumulate have raised significant public health concerns. In particular, PFAS exposure has been associated with weakened immune responses after vaccination, including reduced immunosuppression biomarkers such as immunoglobulin production (Luoping Zhang. et al., 2022). Studies have highlighted the connection between PFAS exposure during pregnancy and immune response in both mothers and children. For example, the Norwegian Mother and Child Cohort Study reported significant inverse associations between the concentrations of maternal blood Perfluorooctanoic acid (PFOA), Perfluorooctanesulfonic acid (PFOS), Perfluorohexanesulfonic acid (PFHxS), and Perfluorononanoic acid (PFNA) measured at delivery, and the levels of anti-rubella antibodies in the children's sera at age three years (Granum B et al., 2013). Given PFAS's known influence on immune function, recent studies have begun exploring how PFAS exposure may impact immune responses to specific infections, including SARS-CoV-2. Indeed, communities exposed to higher levels of PFAS exhibited higher odds of COVID-19 mortality (Catelan D et al., 2021). Moreover, elevated plasma levels of perfluorobutanoic acid (PFBA) have been found to be associated with more severe SARS-CoV-2 infections (P Grandjean, 2020), while higher serum levels of PFOS, PFHxS, PFNA have been linked to a weaker antibody response after SARS-CoV-2 infection (Hollister J, 2023). Our team previously found that levels of a mixture of PFASs, including n-PFOA, PFHxS, perfluoroheptanesulfonic acid (PFHpS), and perfluorohexanoic acid (PFHxA), were inversely associated with maternal SARS-CoV-2 IgG (IgG) antibody levels in pregnant individuals (K. Kaur et al., 2023). However, the underlying biological mechanisms are not yet fully understood.

Metabolomics, representing the final products of biochemical changes and closest omics layer to disease and health phenotypes, has advanced rapidly with developments of high-resolution mass spectrometry (HRMS) which can simultaneously measure tens of thousands of endogenous and exogenous metabolites representing a range of biologically relevant pathways for discovery. To understand the disease's pathophysiology and potential therapeutic strategies, several studies have investigated the immune response and metabolic signatures in SARS-CoV-2 patients (Song JW, et al., 2020; Thomas T, et al., 2020; Gardinassi LG,et al., 2020; Takeshita H, et al., 2022; Valdés A, et al.,2022). Furthermore, as endogenous metabolites have previously been associated with PFAS exposures (India-Aldana S, et al., 2023), disrupted biological pathways are considered as potential mediators linking exposures to diverse health outcome (Wei, M., et al., 2021; Mallol R, et al., 2021).

Traditional mediation analysis methods (Baron and Kenny, 1986) are designed to decompose the total effect of an exposure on an outcome into direct and indirect effects through mediators. However, these methods are generally limited to single-exposure, single-mediator scenarios (Valeri and VanderWeele, 2013; Daniel RM, et al., 2015) and struggle with high-dimensional data, particularly when mediators are highly correlated. In studies involving numerous, interrelated metabolites, individual mediation analysis is not only computationally expensive but also risks inflating the multiple comparison error. This complexity underscores the need for an approach that can efficiently summarize multiple correlated metabolites into an "interpretable index," capturing their joint effects on the outcome. For instance, several comprehensive approaches have been developed to focus on generating latent factors through dimensionality reduction techniques, such as principal component analysis (PCA) (Huang and Pan, 2016; Goodrich, et al., 2024) and partial least squares (PLS) (Assi N, et al., 2018). These methods transform correlated mediators into independent latent factors that may represent molecular pathways, followed by mediation analysis on these factors. Weighted Quantile Sum (WQS) regression (Carrico, C, et al., 2013) as a mixture modeling tool offers a practical and effective solution by aggregating metabolites into indices, thus reducing dimensionality while preserving interpretable insights. WQS can efficiently handle both positive and negative metabolite indices, making it particularly suited to our study, where metabolite levels can be increasing or decreasing in

the link between PFAS exposures and IgG levels. By creating these mixture indices, WQS not only reduces the high computational burden but also addresses the challenge of multiple comparisons, allowing for a robust assessment of the overall metabolite effects within a comprehensive framework.

In this study, we profiled the plasma metabolome in the same individuals as our previous study (K. Kaur et al., 2023) and conducted mediation analysis. We applied WQS in a mediation analysis integrating high-dimensional plasma metabolomics and PFAS mixture exposures to provide insights on the biological impacts of PFAS exposures linked to IgG response in pregnant individuals.

Methods

Study Population

The Generation C cohort was created to explore the impact of SARS-CoV-2 infection on pregnancy and birth outcomes in pregnant individuals. A total of 3,157 pregnant individuals were enrolled from April 20, 2020 until Feb 24, 2022. They met the eligibility criteria of being 18 years or older, receiving obstetrical care at Mount Sinai Health System, having a single live birth, and residing in NYC. As part of their routine obstetrical care, blood samples were collected from participants, following informed consent. Past SARS-CoV-2 infection was verified through a serological IgG antibody test and a review of their electronic medical records (EMR) (Gigase et al., 2024; Janevic et al., 2022; Lesseur et al., 2022). Procedures were approved by the institutional review board at the Icahn School of Medicine at Mount Sinai. We previously reported an inverse relationship between PFAS and IgG levels in 72 participants with available PFAS and IgG antibody data (K. Kaur et al., 2023). For the follow-up study, we measured the metabolome in a subset of these individuals with sufficient plasma remaining (N=59).

Covariates

For each participant, demographic variables including maternal age, race/ethnicity, pre-pregnancy body mass index (BMI), gestational age at blood draw, parity, as well as the number of administered COVID-19 vaccine doses prior to blood draw. We also included the type of insurance as a measure of socioeconomic status. Cohort demographics and clinical characteristics of the 59 Generation C participants in this study are summarized in Table 1.

Maternal Plasma PFAS Measurements

Maternal plasma PFAS measurements have been described previously (K. Kaur et al., 2023). In brief, maternal plasma samples, were stored at −80°C and analyzed for 16 PFAS congeners using a low-volume (100 µL) and high-sensitivity (0.2 ng/mL LOD) isotope-dilution LC-MS/MS assay at the Icahn School of Medicine at Mount Sinai's Human Health Exposure Analysis Resource (HHEAR) Targeted Analysis Laboratory. The laboratory adheres to internal quality assurance protocols and participates in proficiency testing programs such as G-EQUAS (https://app.g-equas.de/web/) (Göen T et al., 2012) and CTQ-AMAP(https://www.inspq.qc.ca/en/ctq/eqas/amap/description) (CTQ, AMAP: AMAP Ring Test for Persistent Organic Pollutants in CTQ, 2022). The method, based on CDC protocols with modifications, quantifies widely studied PFAS (n-PFOS, Sm-PFOS, n-PFOA, PFHxS, PFNA, and PFDA), emerging PFAS (PFBS, PFHpS, PFHpA, PFHxA, PFUnDA, and PFDoDA), and replacements (N-EtFOSAA and N-MeFOSAA). For PFAS concentrations below the limit of detection (LOD), values were estimated as LOD/(√2). PFAS compounds detected below the LOD in more than 40% of samples were excluded. The final analysis focused on nine PFAS compounds: PFOS, PFHxA, PFHxS, n-PFOA, PFHpS, PFDA, PFNA, PFBS, and PFUnDA. ngeners (PFOS, PFHxA, PFHxS, n-PFOA, PFHpS, PFDA, PFNA, PFBS, and PFUnDA).

SARS-Cov-2 IgG antibody quantification

Serological testing for quantifying IgG antibodies against the SARS-CoV-2 spike (S) protein was performed with an enzyme-linked immunosorbent assay (ELISA) developed at the Icahn School of Medicine at Mount Sinai (Stadlbauer et al., 2020). Results are reported as antibody units per milliliter (AU/mL).

Maternal Plasma Metabolites Analysis

Plasma metabolomics was performed with LC-HRMS using established protocols (Hua X et al., 2023; Niedzwiecki MM et al., 2021; Yu M et al., 2024). For each sample, 50 µL of plasma was combined with 150 µL of ice-cold methanol crash solution, vortexed for 10 seconds, incubated at -80 °C for 30 minutes, and centrifuged at 13,000g for 15 minutes at 4 °C. The samples were then evaporated using a Savant SC250EXP SpeedVac vacuum concentrator at 35 °C for 90 minutes. Dried sample extracts were stored at -80 °C. Pooled quality control (QC) samples were created by combining 20 µL extracts from each plasma sample. In the same extraction process, solvent blanks were prepared by substituting plasma with water. The samples were analyzed in a randomized sequence, with pooled QCs injected every 10 samples throughout the run. Procedural blank extracts were analyzed three times at the start and end of the batch. The samples were analyzed in one batch by ultra-performance liquid chromatography coupled to a HRMS in both reverse-phase (RP) positive and negative ionization modes and Zwitterion Hydrophilic Interaction Chromatography (HILIC) chromatography in positive ionization mode. Metabolite identifications were made using our local database, which comprises over 1000 biologically and environmentally relevant reference standards analyzed under the same conditions. Matching involved considering retention time (± 8 sec), accurate mass (< 20ppm), isotope distribution, and MS/MS fragmentation pattern (when available) against the in-house Personal Chemical Database Library and Profinder software (Agilent Technologies, Santa Clara, USA), resulting in annotation confidence levels 1 and 2 (Schymanski EL, 2014). Metabolite classes were determined using ClassyFire (Djoumbou Feunang et al., 2016).

Annotated metabolites in each of the three modes were filtered and normalized. An 80% missing value threshold was set and metabolites exceeding this threshold across samples were excluded from further analysis. Only metabolites above a signal-to-noise threshold of 1.5 median signal fold change in samples compared to solvent blank were maintained. To correct the batch effects, all metabolites were corrected using TIGERr (Siyu Han et al., 2022). A quality criteria threshold of 30% coefficient of variation (CV) in repeated injections of pooled QC samples was set to eliminate metabolites with high variability. We then combined the cleaned and normalized metabolites of the three modes and eliminated any duplicates (see **Figure S2**), giving priority to the analysis mode with higher abundance and lower missingness. Subsequently, a log2 transformation was applied to the remaining metabolite values to normalize the data and facilitate statistical comparisons. We then imputed the missing values by using a 2- step mechanism with the package “Mechanism-Aware Imputation (MAI)” (Dekermanjian, J.P. et al, 2022). Finally, all values were standardized in z-score for downstream statistical analysis.

Statistical Analysis

In this study, all analyses were adjusted for maternal age, maternal race/ethnicity, parity, type of insurance, gestational age at blood draw (weeks), receipt of the COVID-19 vaccine before blood collection, and pre-pregnancy BMI. We first conducted univariate linear regression analysis for each individual PFAS congener to assess its association with IgG levels. Following this, we used WQS regression (Carrico, C, et al., 2013) to estimate the combined mixture effect of 9 PFAS exposures on IgG levels in the adverse direction by creating a single outcome-related index, called the PFAS-index. This analysis was restricted to the negative

direction based on our previous findings in a larger population of 72 individuals (K. Kaur et al., 2023). We then used a random-subset implementation of WQS (WQS_{RS}) appropriate for highly collinear omics contexts (Curtin, P. et al., 2019) to identify an index and assess the combined impact of metabolites. Two indices were constructed to capture distinct associations between metabolite levels and IgG. The first index [metabolites-index (Neg)] includes metabolites whose decreased plasma levels are associated with IgG, while the second [metabolites-index (Pos)] includes those whose increased levels are associated with lower IgG. This separation allows us to capture both positive and negative relationships, reflecting potentially distinct biological pathways. In this step, each metabolite within the index was weighted based on its contribution to the observed association, which was estimated through bootstrapping (n=3,000).

To further examine whether either direction of the metabolites-index could potentially mediate the association between the PFAS-index and the IgG antibody levels, we implemented the mediation analysis using the R package "lavaan". In the single mediator analysis, it involves regressing the metabolites-index on the PFAS-index and covariates in the mediator model, and regressing IgG antibody levels on the PFAS-index, metabolites-index, and covariates in the outcome model. Together, these models estimate the direct and indirect effects of the PFAS-index on IgG levels. To study the combined effect of the two metabolic-indices, we also employed a multiple-mediator analysis. To obtain robust standard errors and the corresponding 95% CIs for the mediation estimates, we employed bias-corrected accelerated bootstrapping to estimate the sampling distribution of parameter estimates with 5000 simulations (Shrout PE. et al., 2002). **Figure S1** is a schematic of the mediation analysis workflow conducted in this study, detailing both univariate and multivariate models that assess the direct and indirect effects of PFAS exposure on IgG levels through specific metabolite indices.

We then performed metabolite set enrichment analyses using the set of metabolites that passed the weight threshold (1/metabolite set size of 286) in both metabolites-indices using the Over Representation Analysis (ORA) in MetaboAnalystR 4.0 (Pang, Z., 2024). The human Kyoto Encyclopedia of Genes and Genomes (KEGG) pathway database was used, statistical significance was based on a p-value threshold of 0.05.

Results

Demographic and clinical characteristics of the study population (N=59) are found in Table 1. The demographic characteristics of this population (N=59) are similar to those in our previous study (N=72). At the time of the blood collection, the average age of the mother was 32.8 years (SD=4.34) and the average gestational age at blood draw was 27.3 weeks (SD=11.0). The participants were nulliparous (55.9%) and multiparous (44.1%). The population included 23.7% (n=14) self-identified as Black, 25.4% (n=15) as Hispanic, 40.7% (n=24) as white, and 10.2% (n=6) as other. Most participants were privately insured (72.9%). Five participants had received at least one COVID-19 vaccine dose before blood collection.

	N (%)	**Mean (SD)**	**Median [Range]**
Pre-pregnancy BMI (kg/m^2)		30.2 (8.23)	28.3 [18.9, 59.8]
Normal	16 (27.1)		
Overweight	18 (30.5%)		
Obese	25 (42.4%)		

Gestational age at blood draw (weeks)		27.3 (11.0)	29.7 [4.71, 39.9]
Maternal age at delivery (years)		32.8 (4.34)	33.0 [24.0, 44.0]
Self-identified Race/Ethnicity			
Black	14 (23.7%)		
Hispanic	15 (25.4%)		
Other	6 (10.2%)		
White	24 (40.7%)		
Parity			
Multiparous	26 (44.1%)		
Nulliparous	33 (55.9%)		
Receipt of the COVID-19 vaccine prior to blood draw			
No	54 (91.5%)		
Yes	5 (8.5%)		
Insurance			
Private/self-pay	43 (72.9%)		
Public	16 (27.1%)		

Table 1: Descriptive characteristics of the population's potential confounding variables in the current study (N=59). Participant characteristics are for the time of blood draw unless otherwise stated.

Following data preprocessing, 284 annotated metabolites were selected for downstream analysis. Summary statistics for those 286 metabolites, based on their $\log_2$-transformed abundances and grouped by metabolite superclass, are presented in **Tables S1** and **Table S2**. Additionally, descriptive statistics for the PFAS-index and two metabolite indices are reported in **Table S3**. The results of linear regression analysis for individual PFASs are provided in the supplementary material (see **Figure S4**).

In the current study, the PFAS-index was inversely associated with IgG (Total Effect= -0.273 (95% CI: -0.433,-0.199), see Supplementary **Table S4**, **Figure S5)**.

In the analysis of single mediator with negative metabolites-index, we found an estimated indirect effect, indicating that for each one-unit increase in the PFAS-index, there is an increase in the metabolites-index by 0.152 units (beta=0.152 (95% CI:0.067,0.262), p<0.001), resulting in a subsequent decrease in the IgG antibody level by $10^{0.877}$ AU/mL (beta=-0.877 (95% CI: -1.239, -0.488), p<0.001) (see **Figure 1.a-c**). As a result, 48.9% (95% CI: [24.7%, 111%]) of the total effect of the PFAS-index on decreased IgG levels could be explained by the indirect effect of the negative metabolites-index (Indirect Effect=-0.134 (95% CI: [-0.271, -0.055]), p=0.008).

Likewise, in the analysis of a single mediator with positive metabolites-index, we found an estimated indirect effect, indicating that for each one-unit increase in the PFAS-index, there is a decrease in the metabolites by 0.118 units (beta=-0.118 (95% CI:[-0.233,-0.020]), p=0.028), resulting in a subsequent decrease in the IgG levels by $10^{1.161}$ AU/mL (beta=1.161 (95% CI: 0.897, 1.410), p<0.001) (see **Figure 1.d-f**). As a result, 50.1% (95% CI: 9.7%, 75.0%) of the total effect of the PFAS-index on IgG could be explained by the indirect effect of the positive metabolites-index (Indirect Effect =-0.137 (95% CI: -0.287,-0.027), p=0.035).

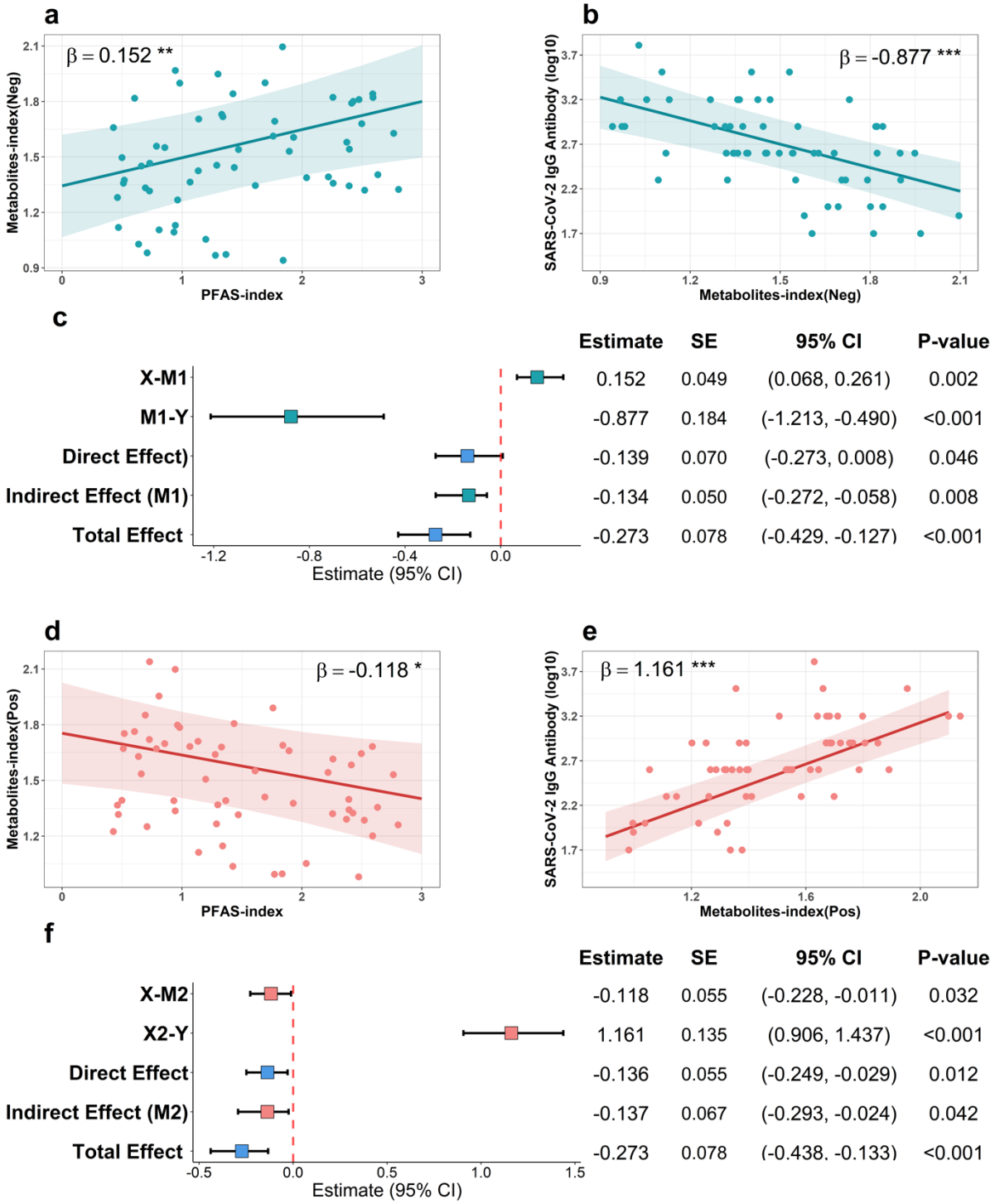

Figure 1: Single mediator analyses for PFAS-index, metabolites-index in the negative direction or metabolites-index in the positive direction, and SARS-CoV-2 IgG antibody levels (N = 59) using models adjusted for maternal age, maternal race/ethnicity, parity, type of insurance, gestational age at blood draw (weeks), receipt of the COVID-19 vaccine before blood collection, and pre-pregnancy BMI. All p-values are estimated using a two-sided test for t-statistics from linear regression models. 95% confidence level (CI) is presented as bias-corrected and accelerated 5,000 bootstrapping. **a)** Scatter plot of the estimated beta (adjusted for the model residual when covariates are included in the model) for the association between the negative direction of metabolites-index and PFAS-index from the mediator model. **b)** Scatter plot of the estimated beta (adjusted for the model residual when covariates are included in the model) for the association between IgG levels and the negative direction of

metabolites-index from the outcome model. **c)** Forest plot of PFAS-index, metabolites-index in the negative direction and SARS-CoV-2 IgG antibody levels mediation analysis summary parameters. **d)** Scatter plot of the estimate estimated beta (adjusted for the model residual when covariates are included in the model) for the association between the positive direction of metabolites-index and PFAS-index from the mediator model. **e)** Scatter plot of the estimated beta (adjusted for the model residual when covariates are included in the model) for the association between IgG levels and the positive direction of metabolites-index from the outcome model. **f)** Forest plot of PFAS-index, metabolites-index in the positive direction and SARS-CoV-2 IgG antibody levels mediation analysis summary parameters. Statistical significance levels for the effects: * ($p < 0.05$); **($p < 0.01$); and ***($p < 0.001$). X (PFAS-index exposure); M1 (Negative Metabolites-Index); M2 (Positive Metabolites-Inde); Y (SARS-CoV-2 IgG levels).

In the joint mediation model adjusting, where both positive and negative metabolite indices are included to control for the mutual influence, we found a significant but smaller indirect effect for both metabolites-indices, 31.5% (95% CI: 15.1%, 76.2%) for the negative metabolites-index (Indirect Effect=-0.086 (95% CI:-0.172,-0.038), p=0.007) and 42.1% (95% CI: 7.8%, 78.6%) for the positive metabolites-index (Indirect Effect=-0.115 (95% CI:-0.248,-0.019), p=0.041), resulting in a cumulative mediation effect of 73.6% (95% CI: 44.9%, 116.4%) (see **Figure 2a**).

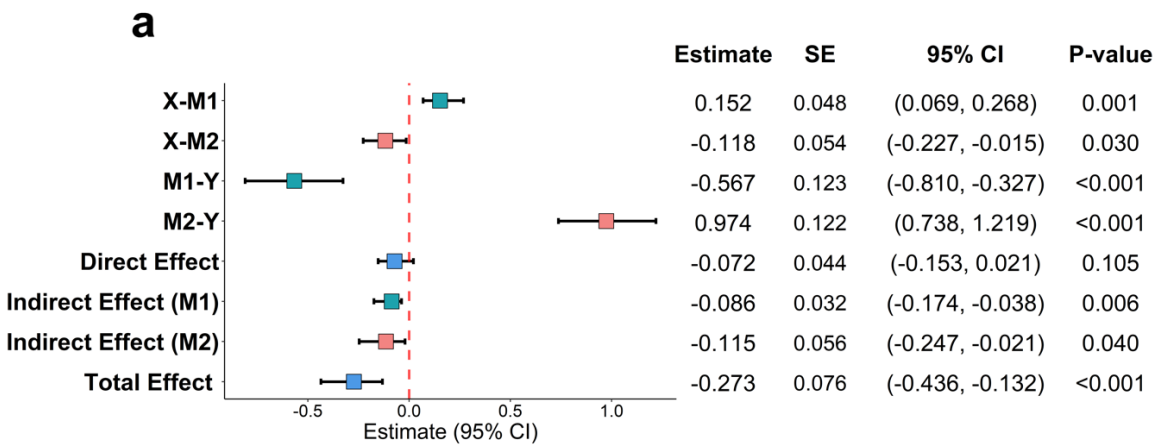

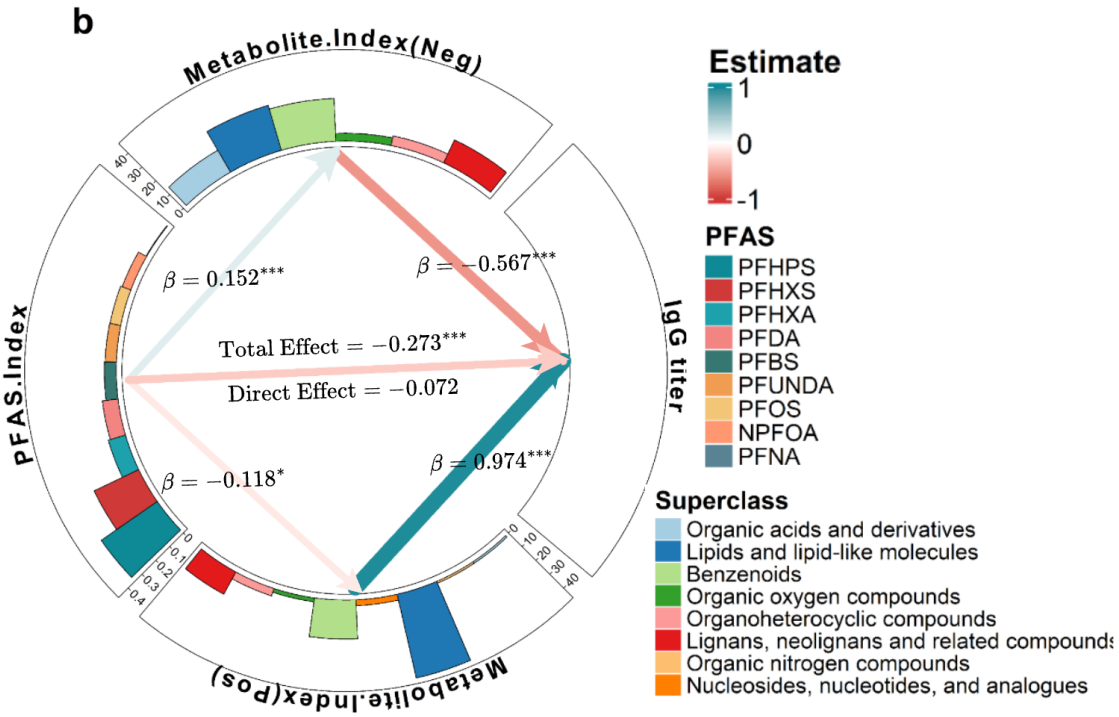

Figure 2: a) Forest plot of joint mediation analysis with two mediators, metabolites-index (Pos) and metabolites-index (Neg), on PFAS-index and SARS-CoV-2 IgG antibody levels (N = 59) adjusted for maternal age, maternal race/ethnicity, parity, type of insurance, gestational age at blood draw (weeks), receipt of the COVID-19 vaccine before blood collection, and pre-pregnancy BMI. All p-values were estimated using a two-sided test for t-statistics from linear regression models, confidence interval. 95% CI is presented as bias-corrected and accelerated 5,000 bootstrapping. X (PFAS-index exposure); M1 (Negative Metabolites-Index); M2 (Positive Metabolites-Inde); Y (SARS-CoV-2 IgG levels). **b)** Circos plot showing the estimates from the joint mediation analysis with two metabolite.indices on the PFAS Index and IgG levels. The thickness of the links between variables represents the strength of the estimates, with the color gradient ranging from red (-1) to turquoise (1) to depict the direction and magnitude of these relationships. Within the PFAS.index sector, the bar plot displays the weights assigned to each PFAS component obtained from the WQS analysis, while the bar plots within the two metabolite indices illustrate the number of chemical superclasses that exceeded the cutoff threshold within each metabolite.index.

In the WQS regression models adjusting for covariates, the metabolite index showed a significant positive association with IgG levels (beta = 1.260, SE = 0.133, $p < 0.001$) and a significant negative association with IgG levels (beta = -0.997, SE = 0.160, $p < 0.001$) (see Supplementary **Table S4**). The weights for the top 10 metabolites that passed the cutoff threshold (1/286) are illustrated in **Figure 3 (**see **Figure S6** for the histogram for the complete list of metabolites that passed the cutoff threshold (1/286) in both indices). Weights indicate the relative contribution of each metabolite to the index. Among the 286 metabolites, plasma N-acetylproline is the most influential compound in the positive association with plasma IgG levels (weight = 0.066) while plasma protoporphyrin is the primary driver in the negative association with plasma IgG levels (weight = 0.032) (see **Figure 3a**). Over half of the metabolites that surpassed the cutoff threshold for the negative metabolite-index were classified as either lipids and lipid-like molecules (24/81) or organic acids and derivatives (22/81). Similarly, 50% of the metabolites surpassing the cutoff for the positive metabolite-index were lipids and lipid-like molecules (44/88), with 13 metabolites classified as organoheterocyclic compounds showing relatively higher weights in this index (see **Figure 2b, Figure S6**).

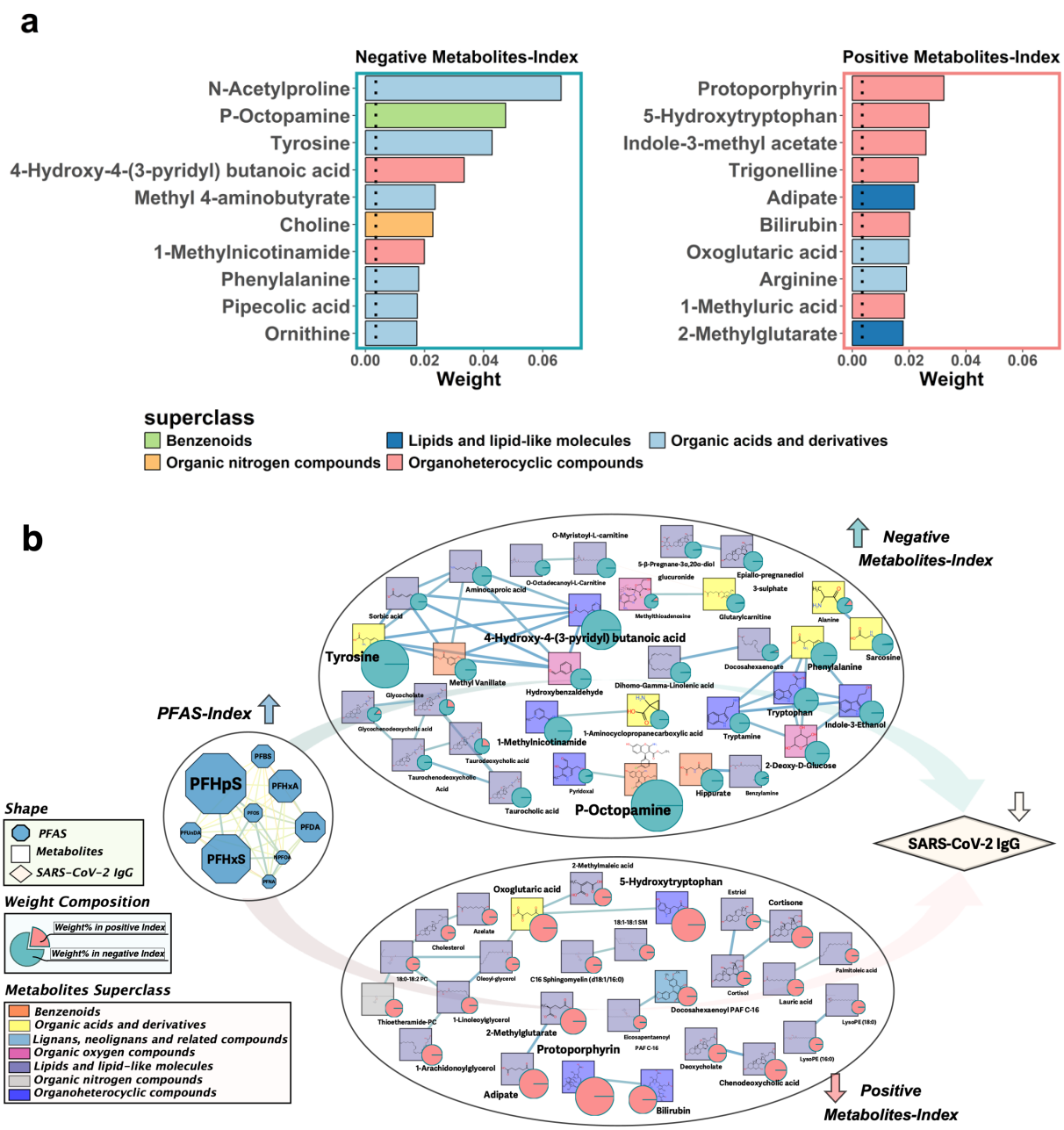

Figure 3: a) Bar graph shows the weights of top 10 metabolites that surpassed the cutoff threshold in negative metabolites-index (left) and positive metabolites-index (right). Weights ordered from the highest weight to the lowest of the negative index. The dotted dark line represents the cutoff (1/286), the color of each bar represents the respective chemical superclass of each metabolite. **b**) The network illustrates the primary contributors within the PFAS-Index and two metabolite indices. Nodes represent different entities: metabolites (rectangles), PFAS exposures (octagons), and SARS-CoV-2 IgG levels (diamond). Metabolites are color-coded according to their chemical superclass, with pie chart size reflecting both their relative weight and composition across the indices. Links between metabolites and PFAS nodes represent their partial correlations.

To characterize the metabolic pathways associated with IgG levels in SARS-CoV-2 positive individuals, we conducted KEGG pathway enrichment analysis (see **Figure 4**). For the 81 metabolites in the negative metabolite-index, seven pathways were significantly enriched (Fisher's $p < 0.05$) with phenylalanine, tyrosine, and tryptophan biosynthesis the most significant pathway. For the 88 metabolites in the positive metabolite-index, several pathways

were also significantly enriched with arginine biosynthesis the most significant pathway. Notably, primary bile acid biosynthesis was significantly enriched in both indices.

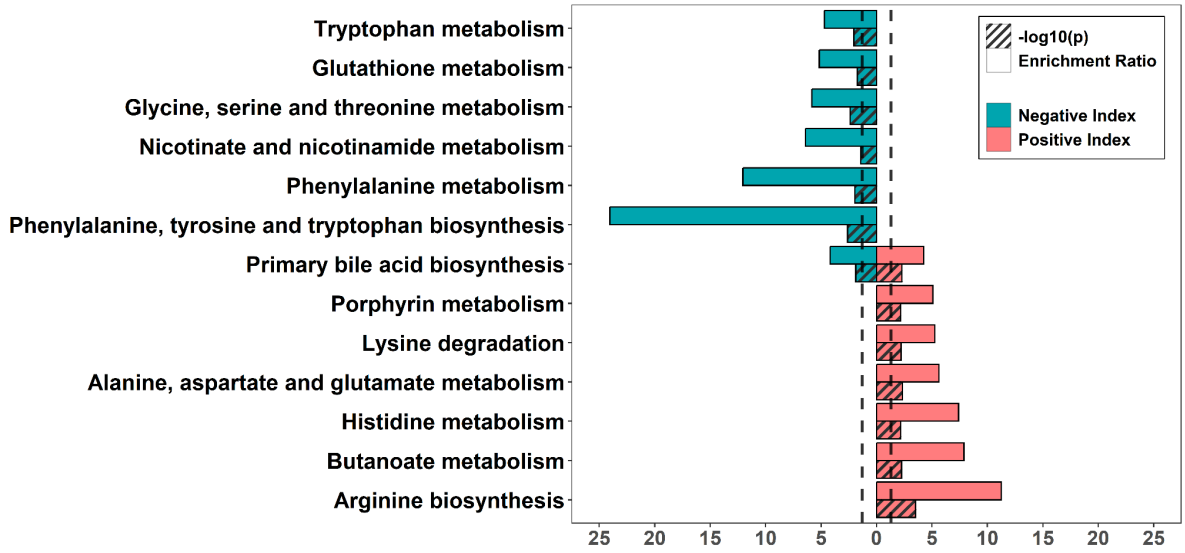

Figure 4: Summary of significantly enriched metabolic pathways (Fisher's p<0.05) from the KEGG database, analyzed using MetaboAnalyst's overrepresentation analysis (ORA). The turquoise bars represent the pathway analysis results using 81 influential metabolites exceeding the cutoff threshold in the negative metabolite index, while the red bars represent results based on 88 influential metabolites from the positive metabolite index. The X-axis displays the identified enriched metabolic pathways, while the Y-axis indicates the corresponding enrichment ratios or -log10 p-values.

To determine whether the mediation effects observed in the PFAS mixture index were consistent with individual PFAS, we extended our analysis to investigate the mediation effects of individual PFASs, focusing specifically on PFHpS and PFHxS, as they contributed most prominently to the calculated PFAS-index (see **Figure S5)** and showed a significant association with IgG levels (see **Figure S4)**. Both metabolites-indices demonstrated significant mediation effects on the association between PFHxS and IgG levels (see **Figure S7**). The total effect was -0.777 (95% CI: [-0.1334, -0.307]), with the negative metabolites-index showing an indirect effect of -0.432 (95% CI: [-0.971, -0.099]) and the positive metabolites-index showing an indirect effect of 0.439 (95% CI: [-0.921, -0.059]) in the analysis of single mediator. In the joint mediation analysis, the negative metabolites-index remained a significant mediation effect of -0.279 (p = 0.023) and the positive metabolites-index had a borderline significant effect of -0.264 (p = 0.051). Using PFHpS (**Figure S8**), results were imprecise suggesting a possible mediation effect in both single and multiple mediators mediation analysis that did not reach significance.

Discussion:

We demonstrate a novel application of WQS in mediation analysis to unravel biological pathways and important metabolites that underlie the previously reported inverse relationship between PFAS exposure and SARS-Cov-2 IgG titer levels. Our results showed that PFAS mixture exposure might disrupt the balance of metabolites, ultimately contributing to a reduced plasma IgG production. This involved two potential mechanisms: increasing metabolite levels linked to lower IgG levels and decreasing metabolite levels associated with higher IgG levels, through distinct and overlapping metabolic pathways.

The aim of this approach was to reduce bias due to collinearity (see **Figure S3**) and estimate the cumulative effect of plasma metabolites associated with IgG levels in both positive and negative directions. As a result, by constructing metabolites indices, we reduced the dimensionality of 286 metabolites to 2, thereby lowering the computational costs and avoiding multiple comparison errors.

The significant mediation effects of the positive and negative WQS indices in both single and multiple mediators analysis suggests that the exposure influences the outcome through different sets of metabolites. Some metabolites may worsen the outcome while others may have a protective effect. In particular, the PFAS-index increases a set of metabolites that are associated with lower SARS-CoV-2 IgG titer levels suggesting that the PFAS-index could be leading to a reduction in IgG levels through this set of metabolites [metabolites index (neg)]. The PFAS-index also decreases a set of metabolites that are associated with higher IgG titer levels suggesting that the exposure could be suppressing metabolites that would normally boost the IgG levels [metabolites index (pos)]. The findings that both metabolites-indices significantly mediate the relationship between PFAS-index and SARS-CoV-2 antibody levels provides insight into how PFAS mixture exposure may influence immune function through multiple metabolic pathways. Specifically, the two indices represent distinct sets of metabolites with different patterns: one index captures metabolites whose levels decrease in association with IgG, while the other captures those that increase. This suggests that PFAS exposure may simultaneously activate or suppress different metabolic processes, each impacting the immune response in a unique way, and these distinct pathways likely reflect complex biological mechanisms by which PFAS interferes with immune function.

In the analysis of the single mediator, the indirect effects of positive and negative metabolite-indices were analyzed separately. The significant results for both the direct and indirect effects suggest that each mediator independently accounts for a portion of the relationship between the PFAS-index and IgG levels. The significant direct effect suggests that, even after considering the mediation effect of the index, part of the total effect remains unexplained by the mediator. Therefore, PFAS exposure might influence IgG levels through multiple metabolic pathways, each with distinct roles in IgG regulation. Conversely, in the joint mediation model, while the indirect effects for both mediators remained significant, the direct effect became non-significant. This shift suggests that when the effects of both indices are considered together, they collectively explain most of the association between the PFAS-index and IgG levels. Furthermore, in the analysis of the single mediator, we observed that 48.9% (95% CI: [24.7%, 111%]) of the effect of PFAS-index on IgG levels was mediated by the negative metabolites-index, and 50.1% (95% CI: [9.7%, 75%]) was mediated by the positive metabolites-index. While in the joint mediation analysis, we adjusted for both metabolites-indices simultaneously and found that the cumulative mediation effect was 73.6% (95% CI: [44.9%, 116.4%]). This suggests that there is likely overlap between the pathways through which each index mediates the link between PFAS-index and IgG levels (VanderWeele TJ, 2014). Enrichment analysis (see **Figure 4**) revealed that primary bile acid biosynthesis was significantly enriched in both indices. Additionally, some pathways, such as taurine and hypotaurine metabolism, were commonly but not significantly enriched in both indices, while others, such as tryptophan metabolism and arginine biosynthesis, were significantly enriched in one direction but not in the other (see **Figure S9**).

The pathway analysis revealed that the majority of significantly enriched pathways were related to amino acid metabolism. The most significantly enriched pathway in the negative metabolites index was phenylalanine, tyrosine, and tryptophan biosynthesis. We found that the two metabolites involved in this pathway, phenylalanine and tyrosine, both had relatively high weights in the index (ranked 8 and 3), and have also been associated with COVID-19 (Troisi J, et al., 2020). Troisi et al. demonstrated an increasing trend in IgG levels from controls to asymptomatic and mild severity patients, whereas tyrosine and phenylalanine concentrations were lower in mildly symptomatic patients compared to both controls and

asymptomatic individuals. Additionally, phenylalanine, tyrosine, and tryptophan biosynthesis has been reported as one of the most common metabolic pathways in metabolomics studies of PFAS exposure (Guo P, 2022, et al., 2024).

Our results also suggest that tryptophan metabolism and kynurenine metabolites play a biological role linking PFAS exposure to IgG titer levels. Metabolites involved in tryptophan metabolism, such as tryptophan, indole-3-pyruvate, tryptamine, and indole-3-acetic acid, were moderately weighted in the negative metabolites index (ranked 14, 28, 29, and 78), indicating that elevated levels of these metabolites are associated with decreased IgG levels. Conversely, kynurenine pathway metabolites (kynurenine and kynurenate), which play crucial roles in the regulation of both innate and adaptive immune responses (Dehhaghi M, 2024; A et al., 2021), were considered as meaningful contributors in the positive metabolites index, with decreased levels of these metabolites associated with decreased IgG levels. These findings align with previous studies (Thomas T, et al., 2020; Gardinassi LG,et al., 2020; Takeshita H, et al., 2022; Valdés A, et al.,2022) where altered tryptophan metabolism into the kynurenine pathway is considered one of the top pathways affected in COVID-19 cases. Specifically, decreased serum tryptophan and indole-3-pyruvate levels, along with increased kynurenine and kynurenate were found in COVID-19 patients compared to healthy individuals (Thomas T, et al., 2020). Moreover, tryptophan levels were found to be decreased in post-acute sequelae of COVID-19 (PASC, “Long COVID”) patients (Wong AC, et al., 2023). Furthermore, tryptophan metabolism is one of the most reported PFAS-associated metabolic pathways (Guo P, et al., 2022). Thus, the significant mediation effects observed in this study suggests that with increased PFAS-index levels, the kynurenine/tryptophan ratio decreased, indicating that less tryptophan was being metabolized through the kynurenine pathway, which could contribute to decreased IgG levels.

Arginine metabolism plays an important role in immune response and was the most significantly enriched pathway in the positive metabolites-index. The levels of arginine available in the body significantly influence the normal functioning of the immune system (Adebayo A, et al., 2021), particularly via supporting the proliferation of T cells (Zhu X, et al., 2014). Exposure to PFAS mixtures may decrease the plasma arginine levels (Congcong Liu, 2023), potentially leading to reduced T cell proliferation and diminished T cell memory response, which results in a weaker immune response, including lower IgG levels.

Finally, the presence of primary bile acid-related metabolites in the negative metabolite-index (such as cholesterol, 25-hydroxycholesterol, chenodeoxycholic acid, taurine, and cholic acid) and in the positive metabolite-index (including glycine, glycochenodeoxycholate, glycocholate, and taurocholate) suggests that the primary bile acids pathway has a complex and dual role in relation to IgG levels. Bile acids are known to impact gut microbiome health and microbial balance, thereby influencing key pathways involved in immune regulation and inflammation (Fiorucci S,et al., 2018). Clinical studies have revealed alterations in bile acid metabolism in COVID-19 patients (Valdés A,et al., 2022). Certain bile acids, such as chenodeoxycholic acid (CDCA), have been shown to activate nuclear receptors like the Farnesoid X receptor (FXR) and the G-protein coupled receptor (TGR5), which regulate glucose, lipid, and energy metabolism and are involved in inflammation and immune responses (Chiang JYL,et al., 2020). However, CDCA has also been found to inhibit IgG production while enhancing intracellular IgG concentration (Correia L, et al., 2001). Furthermore, exposure to PFAS may disrupt the balance of bile acids, altering the metabolic profile in ways that could impair immune function (Guo P, et al., 2022). Individual PFAS increases cholesterol levels and enhances bile acid uptake in the gut, potentially promoting inflammation and leading to cellular stress and damage that could impair immune responses (Behr AC, et al., 2020; Salihović S, et al., 2019).

In the mediation analysis of metabolites-indices on individual PFAS and IgG, we observed a significant mediation effect on PFHxS and IgG levels. However, PFHpS, despite being the

most significantly associated with IgG levels and carrying the highest weight in the PFAS-index, did not show a significant effect. This highlights the complexity of PFAS mixture effects. It suggests that PFHxS may be more directly involved in the biological pathway that influences IgG levels through the constructed metabolites mixture indices. PFHpS, on the other hand, may mediate its effects through a different mechanism that does not involve the same mediators as PFHxS, i.e., PFHpS may contribute to IgG levels through alternative mechanisms not fully captured in the current metabolomics assay. Further research should include lipidomics or alternative molecular assays to explore the potential alternative mechanisms through which PFHpS affects IgG levels.

The primary limitation of this study is its small sample size. However, as a preliminary investigation, the key metabolic pathways identified in our two metabolite indices have been thoroughly studied in previous research on PFAS exposures and SARS-CoV-2, and our findings are consistent with those studies. To assess the power of detecting a mediation effect based on Sobel's test, we utilized the R library "powerMediation" (Weiliang Qiu, et al., 2021). It yielded a power of 0.821 for testing the individual mediation effect of metabolites-index (Neg) and 0.706 for metabolites-index (Pos), indicating a 82.1% and 70.6% probability of correctly rejecting the null hypothesis of no mediation effect at the significance level p=0.05. Further studies should consider increasing the sample size to enhance the study's power. Our study is cross-sectional by nature, thus no causal inference can be made (Winer ES, et al., 2016). Therefore, the observed mediation effects of metabolites-indices on PFAS mixture and IgG levels should be interpreted with caution due to the small sample size and cross-sectional nature of the study.

Conclusions:

In summary, our study presented a novel application of WQS in mediation analysis, simplifying the complexity of high-dimensional metabolomics data by consolidating them into two indices. Our analysis demonstrates that PFAS exposures may reduce IgG levels through potential mechanisms that involve both increasing metabolite levels linked to lower IgG levels and decreasing metabolite levels associated with higher IgG levels, with distinct and overlapping pathways contributing to these effects. To confirm these results and gain a deeper understanding of the causal mechanisms, future research should include larger cohorts with longitudinal desings. Overall, these results suggest potential biological pathways in support of immunotoxicity of PFAS. This study offers a valuable analytical approach for identifying the metabolic effects linking exposure-outcome associations to enhance causal inference in observational studies.

Author contributions:

Conceptualization: H.G., J.C. and L.P.

Funding acquisition and Methodology: J.C. and L.P.

Investigation: J.C. and L.P.

Experiments: G.D.

Formal analysis: H.G., J.C. and L.P.

Supervision: J.C. and L.P.

Original draft: H.G., J.C. and L.P.

Review and editing: All authors

All authors read and approved of the final manuscript.

Funding sources:

We are grateful for support from the National Institutes of Health grants P30ES023515 and UL1TR004419 and HHEAR U2CES030859 and U2CES026561 and R01HD109613. The Generation C study was partially funded by the US Centers for Disease Control and Prevention (CDC) (contract 75D30120C08186). The NIEHS Human Health Exposure Analysis Resource (HHEAR) NIH 2U2CES026561 funded the PFAS measurements, which were carried out within the Senator Frank R. Lautenberg Environmental Health Sciences Laboratory at the Icahn School of Medicine at Mount Sinai. The NIEHS T32HD049311 funded by K. Kaur.

Declaration of competing interest:

The authors declare no conflict of interest.

Acknowledgments:

The authors thank the Generation C team, for collecting and processing biospecimens; Dr. Florian Krammer and his laboratory members for the COVID-19 antibody assay and results.

References:

1. Zhang L, Louie A, Rigutto G, Guo H, Zhao Y, Ahn S, Dahlberg S, Sholinbeck M, Smith MT. A systematic evidence map of chronic inflammation and immunosuppression related to per- and polyfluoroalkyl substance (PFAS) exposure. Environ Res. 2023 Mar 1;220:115188. doi: 10.1016/j.envres. 2022.115188. Epub 2022 Dec 30. PMID: 36592815; PMCID: PMC10044447.
2. Granum B, Haug LS, Namork E, Stølevik SB, Thomsen C, Aaberge IS, van Loveren H, Løvik M, Nygaard UC. Pre-natal exposure to perfluoroalkyl substances may be associated with altered vaccine antibody levels and immune-related health outcomes in early childhood. J Immunotoxicol. 2013 Oct-Dec;10(4):373-9. doi: 10.3109/1547691X.2012.755580. Epub 2013 Jan 25. PMID: 23350954.
3. Catelan D, Biggeri A, Russo F, Gregori D, Pitter G, Da Re F, Fletcher T, Canova C. Exposure to Perfluoroalkyl Substances and Mortality for COVID-19: A Spatial Ecological Analysis in the Veneto Region (Italy). Int J Environ Res Public Health. 2021 Mar 8;18(5):2734. doi: 10.3390/ijerph18052734. PMID: 33800362; PMCID: PMC7967461.
4. Grandjean P, Timmermann CAG, Kruse M, Nielsen F, Vinholt PJ, Boding L, Heilmann C, Mølbak K. Severity of COVID-19 at elevated exposure to perfluorinated alkylates. medRxiv [Preprint]. 2020 Oct 26:2020.10.22.20217562. doi: 10.1101/2020.10.22.20217562. Update in: PLoS One. 2020 Dec 31;15(12):e0244815. doi: 10.1371/journal.pone.0244815. PMID: 33140071; PMCID: PMC7605584.
5. Hollister J, Caban-Martinez AJ, Ellingson KD, Beitel S, Fowlkes AL, Lutrick K, Tyner HL, Naleway AL, Yoon SK, Gaglani M, Hunt D, Meece J, Mayo Lamberte J, Schaefer Solle N, Rose S, Dunnigan K, Khan SM, Kuntz JL, Fisher JM, Coleman A, Britton A, Thiese MS, Hegmann KT, Pavuk M, Ramadan FA, Fuller S, Nematollahi A, Sprissler R, Burgess JL. Serum per- and polyfluoroalkyl substance concentrations and longitudinal change in post-infection and post-vaccination SARS-CoV-2 antibodies. Environ Res. 2023 Dec 15;239(Pt 1):117297. doi: 10.1016/j.envres.2023.117297. Epub 2023 Oct 8. PMID: 37816422; PMCID: PMC10842580.

6. Kaur K, Lesseur C, Chen L, Andra SS, Narasimhan S, Pulivarthi D, Midya V, Ma Y, Ibroci E, Gigase F, Lieber M, Lieb W, Janevic T, De Witte LD, Bergink V, Rommel AS, Chen J. Cross-sectional associations of maternal PFAS exposure on SARS-CoV-2 IgG antibody levels during pregnancy. Environ Res. 2023 Feb 15;219:115067. doi: 10.1016/j.envres.2022.115067. Epub 2022 Dec 14. PMID: 36528042; PMCID: PMC9747685.
7. Colicino E, Pedretti NF, Busgang SA, Gennings C. Per- and poly-fluoroalkyl substances and bone mineral density: Results from the Bayesian weighted quantile sum regression. Environ Epidemiol. 2020 Apr 30;4(3):e092. doi: 10.1097/EE9.0000000000000092. PMID: 32613152; PMCID: PMC7289141.
8. Song JW, Lam SM, Fan X, Cao WJ, Wang SY, Tian H, Chua GH, Zhang C, Meng FP, Xu Z, Fu JL, Huang L, Xia P, Yang T, Zhang S, Li B, Jiang TJ, Wang R, Wang Z, Shi M, Zhang JY, Wang FS, Shui G. Omics-Driven Systems Interrogation of Metabolic Dysregulation in COVID-19 Pathogenesis. Cell Metab. 2020 Aug 4;32(2):188-202.e5. doi: 10.1016/j.cmet.2020.06.016. Epub 2020 Jun 24. PMID: 32610096; PMCID: PMC7311890.
9. Thomas T, Stefanoni D, Reisz JA, Nemkov T, Bertolone L, Francis RO, Hudson KE, Zimring JC, Hansen KC, Hod EA, Spitalnik SL, D'Alessandro A. COVID-19 infection alters kynurenine and fatty acid metabolism, correlating with IL-6 levels and renal status. JCI Insight. 2020 Jul 23;5(14):e140327. doi: 10.1172/jci.insight.140327. PMID: 32559180; PMCID: PMC7453907.
10. Gardinassi LG, Souza COS, Sales-Campos H, Fonseca SG. Immune and Metabolic Signatures of COVID-19 Revealed by Transcriptomics Data Reuse. Front Immunol. 2020 Jun 26;11:1636. doi: 10.3389/fimmu.2020.01636. PMID: 32670298; PMCID: PMC7332781.
11. Takeshita H, Yamamoto K. Tryptophan Metabolism and COVID-19-Induced Skeletal Muscle Damage: Is ACE2 a Key Regulator? Front Nutr. 2022 Apr 8;9:868845. doi: 10.3389/fnut.2022.868845. PMID: 35463998; PMCID: PMC9028463.
12. Valdés A, Moreno LO, Rello SR, Orduña A, Bernardo D, Cifuentes A. Metabolomics study of COVID-19 patients in four different clinical stages. Sci Rep. 2022 Jan 31;12(1):1650. doi: 10.1038/s41598-022-05667-0. PMID: 35102215; PMCID: PMC8803913.
13. India-Aldana S, Yao M, Midya V, Colicino E, Chatzi L, Chu J, Gennings C, Jones DP, Loos RJF, Setiawan VW, Smith MR, Walker RW, Barupal D, Walker DI, Valvi D. PFAS Exposures and the Human Metabolome: A Systematic Review of Epidemiological Studies. Curr Pollut Rep. 2023 Sep;9(3):510-568. doi: 10.1007/s40726-023-00269-4. Epub 2023 Jun 29. PMID: 37753190; PMCID: PMC10520990.
14. Wei, M., Zhao, L., Lv, J. et al. The mediation effect of serum metabolites on the relationship between long-term smoking exposure and esophageal squamous cell carcinoma. BMC Cancer 21, 415 (2021). https://doi.org/10.1186/s12885-021-08151-6
15. Mallol R, Vallvé JC, Solà R, Girona J, Bergmann S, Correig X, Rock E, Winklhofer-Roob BM, Rehues P, Guardiola M, Masana L, Ribalta J. Statistical mediation of the relationships between chronological age and lipoproteins by nonessential amino acids in healthy men. Comput Struct Biotechnol J. 2021 Nov 18;19:6169-6178. doi: 10.1016/j.csbj.2021.11.022. PMID: 34900130; PMCID: PMC8632714.
16. Baron RM, Kenny DA. The moderator-mediator variable distinction in social psychological research: conceptual, strategic, and statistical considerations. J Pers Soc Psychol. 1986 Dec;51(6):1173-82. doi: 10.1037//0022-3514.51.6.1173. PMID: 3806354.
17. Valeri L, Vanderweele TJ. Mediation analysis allowing for exposure-mediator interactions and causal interpretation: theoretical assumptions and implementation with SAS and SPSS macros. Psychol Methods. 2013 Jun;18(2):137-50. doi: 10.1037/a0031034. Epub 2013 Feb 4. Erratum in: Psychol Methods. 2013 Dec;18(4):474. PMID: 23379553; PMCID: PMC3659198.

18. Daniel RM, De Stavola BL, Cousens SN, Vansteelandt S. Causal mediation analysis with multiple mediators. Biometrics. 2015 Mar;71(1):1-14. doi: 10.1111/biom.12248. Epub 2014 Oct 28. PMID: 25351114; PMCID: PMC4402024.
19. Huang YT, Pan WC. Hypothesis test of mediation effect in causal mediation model with high-dimensional continuous mediators. Biometrics. 2016 Jun;72(2):402-13. doi: 10.1111/biom.12421. Epub 2015 Sep 28. PMID: 26414245.
20. Goodrich JA, Wang H, Jia Q, Stratakis N, Zhao Y, Maitre L, Bustamante M, Vafeiadi M, Aung M, Andrušaitytė S, Basagana X, Farzan SF, Heude B, Keun H, McConnell R, Yang TC, Siskos AP, Urquiza J, Valvi D, Varo N, Småstuen Haug L, Oftedal BM, Gražulevičienė R, Philippat C, Wright J, Vrijheid M, Chatzi L, Conti DV. Integrating Multi-Omics with environmental data for precision health: A novel analytic framework and case study on prenatal mercury induced childhood fatty liver disease. Environ Int. 2024 Aug;190:108930. doi: 10.1016/j.envint.2024.108930. Epub 2024 Aug 3. PMID: 39128376.
21. Assi N, Thomas DC, Leitzmann M, Stepien M, Chajès V, Philip T, Vineis P, Bamia C, Boutron-Ruault MC, Sandanger TM, Molinuevo A, Boshuizen HC, Sundkvist A, Kühn T, Travis RC, Overvad K, Riboli E, Gunter MJ, Scalbert A, Jenab M, Ferrari P, Viallon V. Are Metabolic Signatures Mediating the Relationship between Lifestyle Factors and Hepatocellular Carcinoma Risk? Results from a Nested Case-Control Study in EPIC. Cancer Epidemiol Biomarkers Prev. 2018 May;27(5):531-540. doi: 10.1158/1055-9965.EPI-17-0649. Epub 2018 Mar 21. PMID: 29563134; PMCID: PMC7444360.
22. Carrico, C., Gennings, C., Wheeler, D.C. et al. Characterization of Weighted Quantile Sum Regression for Highly Correlated Data in a Risk Analysis Setting. JABES 20, 100–120 (2015). https://doi.org/10.1007/s13253-014-0180-3
23. Gigase FAJ, Jessel RH, Kaplowitz E, Boychuk N, Ohrn S, Ibroci E 1st, Castro J, Lynch J, Tubassum R, Balbierz A, Molenaar NM, Graziani M, Missall R, Flores T, Stern T, Carreno JM; Krammer Serology Core Study Group; Krammer F, Adler A, Brody RI, Lesseur C, Chen J, Ellington S, Galang RR, Snead MC, Howell E, Stone J, Bergink V, Dolan S, Lieb W, Rommel AS, de Witte LD, Janevic T. SARS-CoV-2 infection, inflammation and birth outcomes in a prospective NYC pregnancy cohort. J Reprod Immunol. 2024 Jun;163:104243. doi: 10.1016/j.jri.2024.104243. Epub 2024 Mar 18. PMID: 38522364; PMCID: PMC11144074.
24. Janevic, T., Lieb, W., Ibroci, E., Lynch, J., Lieber, M., Molenaar, N.M., Rommel, A.S., de Witte, L., Ohrn, S., Carreno, J.M., Krammer, F., Zapata, L.B., Snead, M.C., Brody, R. I., Jessel, R.H., Sestito, S., Adler, A., Afzal, O., Gigase, F., Missall, R., Carrion, D., Stone, J., Bergink, V., Dolan, S.M., Howell, E.A., Krammer Serology Core Study, G., 2022. The influence of structural racism, pandemic stress, and SARS-CoV-2 infection during pregnancy with adverse birth outcomes. Am J Obstet Gynecol MFM 4 (4), 100649. https://doi.org/10.1016/j.ajogmf.2022.100649.
25. Lesseur, C., Jessel, R.H., Ohrn, S., Ma, Y., Li, Q., Dekio, F., Brody, R.I., Wetmur, J.G., Gigase, F.A.J., Lieber, M., Lieb, W., Lynch, J., Afzal, O., Ibroci, E., Rommel, A.S., Janevic, T., Stone, J., Howell, E.A., Galang, R.R., Dolan, S.M., Bergink, V., De Witte, L.D., Chen, J., 2022. Gestational SARS-CoV-2 infection is associated with placental expression of immune and trophoblast genes. Placenta 126, 125–132. https://doi.org/10.1016/j.placenta.2022.06.017.
26. Göen T, Schaller KH, Drexler H. External quality assessment of human biomonitoring in the range of environmental exposure levels. Int J Hyg Environ Health. 2012 Feb;215(2):229-32. doi: 10.1016/j.ijheh.2011.08.012. Epub 2011 Sep 19. PMID: 21937272.
27. Ctq A.M.A.P. CTQ; 2022. AMAP Ring Test for Persistent Organic Pollutants in Human Serum 2022.https://www.inspq.qc.ca/en/ctq/eqas/amap/description
28. Stadlbauer D, Amanat F, Chromikova V, Jiang K, Strohmeier S, Arunkumar GA, Tan J, Bhavsar D, Capuano C, Kirkpatrick E, Meade P, Brito RN, Teo C, McMahon M, Simon V, Krammer F. SARS-CoV-2 Seroconversion in Humans: A Detailed Protocol for a Serological Assay, Antigen Production, and Test Setup. Curr Protoc Microbiol.

2020 Jun;57(1):e100. doi: 10.1002/cpmc.100. PMID: 32302069; PMCID: PMC7235504.
29. Hua X, Ungaro RC, Petrick LM, Chan AT, Porter CK, Khalili H; Nurses' Health Study; PREDICTS Collaborators. Inflammatory Bowel Disease Is Associated With Prediagnostic Perturbances in Metabolic Pathways. Gastroenterology. 2023 Jan;164(1):147-150.e2. doi: 10.1053/j.gastro.2022.09.007. Epub 2022 Sep 17. PMID: 36122699; PMCID: PMC9771951.
30. Niedzwiecki MM, Eggers S, Joshi A, Dolios G, Cantoral A, Lamadrid-Figueroa H, Amarasiriwardena C, Téllez-Rojo MM, Wright RO, Petrick L. Lead exposure and serum metabolite profiles in pregnant women in Mexico City. Environ Health. 2021 Dec 10;20(1):125. doi: 10.1186/s12940-021-00810-2. PMID: 34893088; PMCID: PMC8665540.
31. Yu M, Li Q, Dolios G, Tu P, Teitelbaum S, Chen J, Petrick L. Active Molecular Network Discovery Links Lifestyle Variables to Breast Cancer in the Long Island Breast Cancer Study Project. Environ Health (Wash). 2024 Apr 18;2(6):401-410. doi: 10.1021/envhealth.3c00218. PMID: 38932753; PMCID: PMC11197006.
32. Schymanski EL, Jeon J, Gulde R, Fenner K, Ruff M, Singer HP, Hollender J. Identifying small molecules via high resolution mass spectrometry: communicating confidence. Environ Sci Technol. 2014 Feb 18;48(4):2097-8. doi: 10.1021/es5002105. Epub 2014 Jan 29. PMID: 24476540.
33. Djoumbou Feunang, Y., Eisner, R., Knox, C. et al. ClassyFire: automated chemical classification with a comprehensive, computable taxonomy. J Cheminform 8, 61 (2016). https://doi.org/10.1186/s13321-016-0174-y
34. Siyu Han, Jialing Huang, Francesco Foppiano, Cornelia Prehn, Jerzy Adamski, Karsten Suhre, Ying Li, Giuseppe Matullo, Freimut Schliess, Christian Gieger, Annette Peters, Rui Wang-Sattler, TIGER: technical variation elimination for metabolomics data using ensemble learning architecture, Briefings in Bioinformatics, Volume 23, Issue 2, March 2022, bbab535, https://doi.org/10.1093/bib/bbab535
35. Dekermanjian, J.P., Shaddox, E., Nandy, D. et al. Mechanism-aware imputation: a two-step approach in handling missing values in metabolomics. BMC Bioinformatics 23, 179 (2022). https://doi.org/10.1186/s12859-022-04659-1
36. Curtin, P., Kellogg, J., Cech, N., & Gennings, C. (2019). A random subset implementation of weighted quantile sum (WQSRS) regression for analysis of high-dimensional mixtures. Communications in Statistics - Simulation and Computation, 50(4), 1119–1134. https://doi.org/10.1080/03610918.2019.1577971
37. Shrout PE, Bolger N. Mediation in experimental and nonexperimental studies: new procedures and recommendations. Psychol Methods. 2002 Dec;7(4):422-45. PMID: 12530702.
38. Pang, Z., Xu, L., Viau, C. et al. MetaboAnalystR 4.0: a unified LC-MS workflow for global metabolomics. Nat Commun 15, 3675 (2024). https://doi.org/10.1038/s41467-024-48009-6
39. VanderWeele TJ, Vansteelandt S. Mediation Analysis with Multiple Mediators. Epidemiol Methods. 2014 Jan;2(1):95-115. doi: 10.1515/em-2012-0010. PMID: 25580377; PMCID: PMC4287269.
40. Troisi J, Cavallo P, Masarone M, et al. Serum metabolomic profile of symptomatic and asymptomatic SARS-CoV-2 infected patients . Research Square; 2020. DOI: 10.21203/rs.3.rs-34085/v1.
41. Guo P, Furnary T, Vasiliou V, Yan Q, Nyhan K, Jones DP, Johnson CH, Liew Z. Non-targeted metabolomics and associations with per- and polyfluoroalkyl substances (PFAS) exposure in humans: A scoping review. Environ Int. 2022 Apr;162:107159. doi: 10.1016/j.envint.2022.107159. Epub 2022 Feb 26. PMID: 35231839; PMCID: PMC8969205.

42. Krupa A, Kowalska I. The Kynurenine Pathway-New Linkage between Innate and Adaptive Immunity in Autoimmune Endocrinopathies. Int J Mol Sci. 2021 Sep 13;22(18):9879. doi: 10.3390/ijms22189879. PMID: 34576041; PMCID: PMC8469440.
43. Dehhaghi M, Heydari M, Panahi HKS, Lewin SR, Heng B, Brew BJ, Guillemin GJ. The roles of the kynurenine pathway in COVID-19 neuropathogenesis. Infection. 2024 May 27. doi: 10.1007/s15010-024-02293-y. Epub ahead of print. PMID: 38802702.
44. Wong AC, Devason AS, Umana IC, Cox TO, Dohnalová L, Litichevskiy L, Perla J, Lundgren P, Etwebi Z, Izzo LT, Kim J, Tetlak M, Descamps HC, Park SL, Wisser S, McKnight AD, Pardy RD, Kim J, Blank N, Patel S, Thum K, Mason S, Beltra JC, Michieletto MF, Ngiow SF, Miller BM, Liou MJ, Madhu B, Dmitrieva-Posocco O, Huber AS, Hewins P, Petucci C, Chu CP, Baraniecki-Zwil G, Giron LB, Baxter AE, Greenplate AR, Kearns C, Montone K, Litzky LA, Feldman M, Henao-Mejia J, Striepen B, Ramage H, Jurado KA, Wellen KE, O'Doherty U, Abdel-Mohsen M, Landay AL, Keshavarzian A, Henrich TJ, Deeks SG, Peluso MJ, Meyer NJ, Wherry EJ, Abramoff BA, Cherry S, Thaiss CA, Levy M. Serotonin reduction in post-acute sequelae of viral infection. Cell. 2023 Oct 26;186(22):4851-4867.e20. doi: 10.1016/j.cell.2023.09.013. Epub 2023 Oct 16. PMID: 37848036; PMCID: PMC11227373.
45. Adebayo A, Varzideh F, Wilson S, Gambardella J, Eacobacci M, Jankauskas SS, Donkor K, Kansakar U, Trimarco V, Mone P, Lombardi A, Santulli G. l-Arginine and COVID-19: An Update. Nutrients. 2021 Nov 5;13(11):3951. doi: 10.3390/nu13113951. PMID: 34836206; PMCID: PMC8619186.
46. Zhu X, Pribis JP, Rodriguez PC, Morris SM Jr, Vodovotz Y, Billiar TR, Ochoa JB. The central role of arginine catabolism in T-cell dysfunction and increased susceptibility to infection after physical injury. Ann Surg. 2014 Jan;259(1):171-8. doi: 10.1097/SLA.0b013e31828611f8. PMID: 23470573.
47. Liu C, Zhu X, You L, Gin KY, Chen H, Chen B. Per/polyfluoroalkyl substances modulate plasmid transfer of antibiotic resistance genes: A balance between oxidative stress and energy support. Water Res. 2023 Jul 15;240:120086. doi: 10.1016/j.watres.2023.120086. Epub 2023 May 18. PMID: 37257295.
48. Fiorucci S, Biagioli M, Zampella A, Distrutti E. Bile Acids Activated Receptors Regulate Innate Immunity. Front Immunol. 2018 Aug 13;9:1853. doi: 10.3389/fimmu.2018.01853. PMID: 30150987; PMCID: PMC6099188.
49. Chiang JYL, Ferrell JM. Bile acid receptors FXR and TGR5 signaling in fatty liver diseases and therapy. Am J Physiol Gastrointest Liver Physiol. 2020 Mar 1;318(3):G554-G573. doi: 10.1152/ajpgi.00223.2019. Epub 2020 Jan 27. PMID: 31984784; PMCID: PMC7099488.
50. Correia L, Podevin P, Borderie D, Verthier N, Montet JC, Feldmann G, Poupon R, Weill B, Calmus Y. Effects of bile acids on the humoral immune response: a mechanistic approach. Life Sci. 2001 Oct 5;69(20):2337-48. doi: 10.1016/s0024-3205(01)01321-2. PMID: 11681621.
51. Behr AC, Kwiatkowski A, Ståhlman M, Schmidt FF, Luckert C, Braeuning A, Buhrke T. Impairment of bile acid metabolism by perfluorooctanoic acid (PFOA) and perfluorooctanesulfonic acid (PFOS) in human HepaRG hepatoma cells. Arch Toxicol. 2020 May;94(5):1673-1686. doi: 10.1007/s00204-020-02732-3. Epub 2020 Apr 6. Erratum in: Arch Toxicol. 2021 Aug;95(8):2891. doi: 10.1007/s00204-021-03089-x. PMID: 32253466; PMCID: PMC8241792.
52. Salihović S, Dickens AM, Schoultz I, Fart F, Sinisalu L, Lindeman T, Halfvarson J, Orešič M, Hyötyläinen T. Simultaneous determination of perfluoroalkyl substances and bile acids in human serum using ultra-high-performance liquid chromatography-tandem mass spectrometry. Anal Bioanal Chem. 2020 Apr;412(10):2251-2259. doi: 10.1007/s00216-019-02263-6. Epub 2019 Nov 23. PMID: 31760452; PMCID: PMC7118038.
53. WeiLiang Qiu. 2021. doi 10.32614/CRAN.package.powerMediation
54. Winer ES, Cervone D, Bryant J, McKinney C, Liu RT, Nadorff MR. Distinguishing Mediational Models and Analyses in Clinical Psychology: Atemporal Associations Do

Not Imply Causation. J Clin Psychol. 2016 Sep;72(9):947-55. doi: 10.1002/jclp.22298. Epub 2016 Mar 31. PMID: 27038095.